

# A MURS Band Digital Quadrature Transmitter with Class-B I/Q Cell Sharing for Long Range IoT Applications

Avish Kosari, Hun-Seok Kim, David D. Wentzloff  
University of Michigan, Ann Arbor, USA

**Abstract**—This paper presents a quadrature digital transmitter operating in the Multi-Use Radio Service (MURS) frequency band for low power and long-range IoT applications. We introduce a narrowband modulation scheme compliant with the MURS band as an alternative solution for low data-rate wide-area coverage. We present a transmitter architecture based on switched-current PA cells that uses a digital class-B input codeword profile in combination with 25% duty cycled LOs to achieve high efficiency at low transmitted power levels. The transmitter is implemented in a 65nm CMOS process and its performance is measured for single-tone and multi-tone transmissions at 5kb/s and 384kb/s, respectively. It operates from a 1.2V supply and delivers a peak efficiency of 41% at a peak output power of 0dBm. The error vector magnitude at 384kb/s is 4.2%.

**Index Terms**—Class-B, digital transmitter, IoT, long-range, low power, MURS band, quadrature transmitter.

## I. INTRODUCTION

THERE are currently several solutions being proposed for long-range connectivity to Internet of Things (IoT) devices for remote-sensing or dense urban environments. SigFox, LoRa, and Cellular providers [1-3] are all deploying wireless networks for low-data rate and low-power applications. However, these technologies utilize unlicensed ISM bands or paid licensed bands where propagation losses and absorption are high. Therefore in order to achieve very long-range transmissions, they use a high uplink transmission power (>13dBm) and high receiver sensitivity values on the order of -140dBm. In order to mitigate these requirements, we propose a transmission scheme using the unlicensed Multi-Use Radio Service (MURS) band to provide a low-power solution for wide-area coverage for the IoT. This enables communication at distances >50km with low power radios by benefiting from the low-loss propagation characteristics at the lower frequencies.

In this paper, we present a long range digital transmitter (Fig. 1) for the MURS band that is frequency and data rate agile, as a low-power solution for remote IoT connectivity in multipath rich environments. Digital transmitters (DTX) heavily rely on signal processing in the digital domain for calibration and programmability. Therefore due to their flexibility to support complex communication standards as well as compact size and high efficiency, a DTX is a suitable candidate for this application. As a low power and

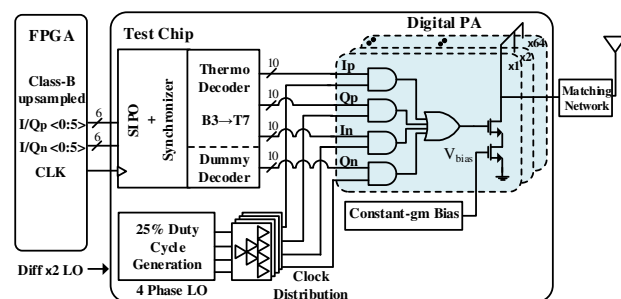


Fig. 1. Block diagram of the digital transmitter.

efficient solution for the IoT long-range connectivity problem, we present a current-mode quadrature digital transmitter architecture that uses the MURS band frequency planning developed in this work. The DTX utilizes 25% duty cycled non-overlapping LO signals combined with a digital class-B code profile for the input I/Q baseband signals, which both improve efficiency. The paper is organized as follows. Section II presents the MURS band transmission scheme and compares it to the existing low power/low-through-put technologies. Section III discusses the existing solutions for digital transmitters and introduces our proposed efficiency enhancement method and quadrature digital transmitter architecture. The design implementation of the digital baseband processing blocks and the DPA will be presented in section IV and the experimental results are discussed in section V.

## II. MURS TRANSMISSION SCHEME

Recently the IoT wireless connectivity problem has been challenged by new types of low-data rate, long-range, technologies mainly operating in sub-GHz frequency bands referred to as low-power WANs (LPWANs). Our goal was to achieve a similar coverage range, while lowering the power consumption in the uplink chain and relaxing the requirements for the downlink, and therefore reducing power on the IoT device. The MURS band is an unlicensed band at 151-154MHz that includes 5 narrowband channels [4]. MURS is similar in regulations to the Family Radio Service (FRS) band used for two-way radios. However, unlike FRS, the FCC allows data communications in the MURS band, for any use, with a limit of 2W transmit power. Based on a link budget analysis, for a transmission range of ~60km and a path loss exponent of 2, we only need to

TABLE I  
MURS CONNECTIVITY COMPARISON WITH LPWAN TECHNOLOGIES

	SIGFOX	LoRa	Ingenu	NB-IoT	MURS
Freq. (MHz)	868/ 902	433/868/915	2400	850/900	151/154
Licensed	No	No	No	Yes	No
Modulation	UNB (DBPSK)	CSS/FSK	RPMA-DSSS	OFDMA/ SC-FDMA	OFDM/ BPSK
Data rate(kb/s)	0.1	0.3-37.5	0.01-8	20-250	5 -384
Coverage range (km)	Rural: 30-50 Urban: 3-10	Rural: 10-15 Urban: 3-5	~15	10-40	LOS: 60
TX P <sub>out</sub>	14dBm	13dBm	20dBm	23dBm	0dBm

transmit 0dBm of power over a narrow bandwidth (5kHz) and require a receiver sensitivity of -110dBm. Therefore relaxing the requirements for the uplink/downlink chains compared to other solutions [1-3].

Table I shows our proposed target specifications and a comparison with other LPWAN technologies using unlicensed bands and the recent NB-IoT technology utilizing licensed bands inside an LTE carrier. In the uplink, we propose both multi-tone and single-tone transmissions. The single-tone transmission is based on either a 10kHz or 5kHz bandwidth, operating at any of the five MURS frequency bands ranging from 151.82MHz to 154.6MHz. To reduce the peak to average power ratio (PAPR), single-tone transmission uses BPSK modulation with data-rates of 5kb/s and 10kb/s. For higher data-rate applications, we propose multi-tone transmission based on 16QAM OFDM with a 10kHz subcarrier spacing and a symbol duration of 125 $\mu$ s (assuming a guard time ratio of 1/4). The OFDM symbols occupy 160kHz of bandwidth over the three lower frequency MURS channels (151.820-151.940MHz) and the 16QAM constellation points are mapped to 16 subcarriers including 12 data, 2 pilot tones and 2 null subcarriers. The data-rate for the multi-tone transmission is 384kb/s. This frequency planning allows realization of a low power multi-mode transmitter enabling long range transmissions for ultra-low-power IoT applications.

### III. DIGITAL TRANSMITTER ARCHITECTURE

#### A. Existing Digital Transmitter Architectures

A number of approaches for digital transmitters have been reported in the literature, including polar, quadrature and out-phasing [5-8]. There are two types of digital power amplifiers (DPA) typically used in these transmitters, one uses switched-current sources and the other type uses voltage-mode switched-capacitors (SC-DPA) for the PA cell. In current-mode DPAs the code-dependent output impedance would introduce AM-AM and AM-PM distortion, however, an ideal peak-to-peak amplitude of  $2 \times V_{DD}$  can be achieved to maximize their output power [8]. The SC-DPAs, on the other hand, have less distortion due to their code-independent impedance but they only have a maximum swing of  $V_{DD}$  at the output. For DTX

architectures, recently, polar architectures have become more popular due to their higher efficiency compared to quadrature architectures. However, polar transmitters require high power consumption and high computation cost due to the use of a CORDIC block for I/Q data to polar conversion, as well as the requirement for accurate timing alignment between phase and amplitude. Therefore quadrature architectures have been studied. The conventional quadrature digital transmitters, as the voltage-mode quadrature architecture proposed in [5], suffer from a lower output power compared to polar transmitters with the same input I/Q magnitude, due to the use of 90° phase shifted digital I/Q LO signals. In [7] three level LO signals have been used to overcome the low efficiency problem for voltage-mode quadrature architectures. In current-mode quadrature DTX as the one in [8], the problem is addressed by using extra I/Q sign bits and two separate DACs for I and Q paths while using the non-overlapping LO signals.

In this work, a digital quadrature architecture is presented that employs switched-current DPAs and uses a digital class-B input code profile in combination with non-overlapping LO signals to overcome the low efficiency problem of conventional quadrature architectures. By employing digital class-B input signals we reduce the number of I/Q DACs to half and eliminate the need for extra processing of the sign bits in current-mode digital quadrature transmitters, therefore improving the efficiency.

#### B. Digital Class-B I/Q Cell Sharing TX Architecture

The block diagram of the MURS band transmitter is shown in Fig. 1. It is based on a low-IF I/Q modulation and all signal processing is performed in the digital domain, preceding the DAC. Motivated by the idea of class-B PAs and with the goal of enhancing the conventional quadrature DTX efficiency, the digital baseband I/Q signals in this design are generated in two pairs of I/Q inputs, namely,  $I_p/Q_p$  and  $I_n/Q_n$ . The baseband signal processing of the quadrature architecture presented in this work is shown in Fig. 2. The digital  $I_p$  and  $Q_p$  data, represent the information for the positive values of baseband I and Q signals, respectively, with the negative values of those signals set to zero and similarly,  $I_n$  and  $Q_n$  codes contain the information for the positive values of the inverted I and Q signals with their negative values set to zero, as shown in Fig. 2(a) and 2(b). The quadrature mixing in this design is performed in the digital domain by mixing the input I and Q data by non-overlapping 25% duty cycled LOs using combinational logic. This topology creates a band pass filter for the up-converted data and also performs image rejection [9].

As shown in Fig. 2(c), at every quarter of the carrier period each of the  $I_p$ ,  $Q_p$ ,  $I_n$ ,  $Q_n$  signals are multiplied by the corresponding  $LO_{1-4}$  to produce the non-overlapping up-converted I/Q signals and therefore for every LO period only one of the  $I_p$ ,  $I_n$ , pair or  $Q_n$ ,  $Q_p$ , pair contains I/Q baseband information with the other one set to zero. The

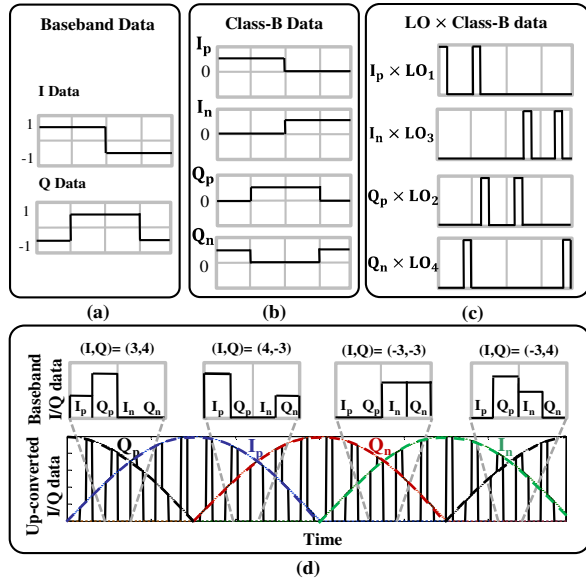


Fig. 2. Baseband signal processing of DTX (a) Baseband I/Q data, (b) Baseband class-B modified I/Q data (c) Up-converted I/Q data, (d) Single tone example of the I/Q combining method.

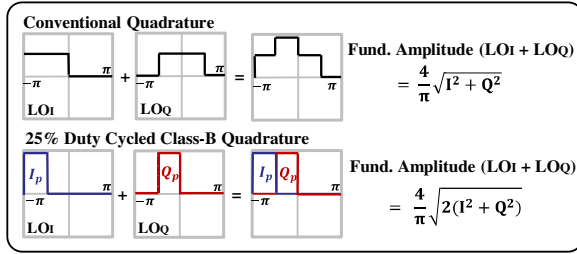


Fig. 3. LO<sub>1</sub>/LO<sub>Q</sub> waveforms and the IQ combined fundamental components in conventional and class-B quadrature TX

up-converted signals are then combined in the time domain to produce the digital form of the modulated signal, therefore the up-converted signal cyclically interchanges between the  $I_p$ ,  $Q_p$ ,  $I_n$ ,  $Q_n$  values. A simple example of a single tone sinusoidal I/Q input data is presented in Fig. 2(d). Combining the digital I/Q data in the digital domain instead of summing them at the output of the DAC is possible in this design since the quadrature signals are never enabled at the same time.

By utilizing the digital class-B coding technique and non-overlapping LOs with a switched-current DPA, we are able to 1) overcome the low output power of conventional quadrature DTX and improve the power of the fundamental RF frequency by 3dB when the power of I and Q inputs are equal, as shown in Fig. 3; 2) achieve an ideal peak-to-peak amplitude of  $2 \times V_{DD}$  at the output of the current-mode DPA with lower power consumption compared to un-coded I/Q inputs; 3) eliminate the need for using I/Q sign bits and two separate DACs for I and Q paths and reducing the number of switch cells to half. Hence an improved efficiency is achieved compared to a conventional quadrature DTX.

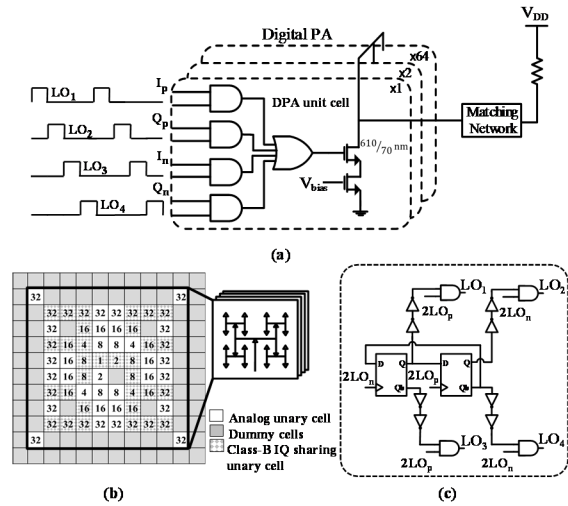


Fig. 4. (a) Class-B IQ cell sharing DPA. (b) Floor plan of the segmented DPA. (c) 25% duty cycle LO generator block.

## IV. DESIGN IMPLEMENTATION

### A. Digital Data Path

As shown in the block diagram of Fig. 1, the digital class-B I/Q baseband signals, which are generated and quantized by 6 bits on an FPGA, are loaded to the chip in a serial mode. The serial-to-parallel converter and the synchronizer align the data to compensate for the delay caused by the code processing. The digital baseband signals are therefore fed to the 16x oversampling DAC at 3.2MHz. In direct RF modulators, such as this work, the quantization noise and aliases reach the output load unfiltered and they can be reduced by increasing the DAC resolution or the sampling rate. By benefiting from the relaxed spectral mask constraints in the MURS band, the selection of this sampling frequency balances the timing constraints and enables a low IF implementation of the transmitter, reducing power consumption in the digital data path. This data is then segmented by a binary to thermometer decoder. The higher three bits are configured in thermometer code and the lower three bits are implemented in binary. Therefore a total of 10 bits of IF data for each of the four I/Q channels reach the mixing DAC, among which there are 7 thermometer-coded and 3 binary bits.

### B. Digital Power Amplifier (DPA)

The DPA is implemented with 6 bits resolution. As shown in Fig. 4(a), each unit cell consists of an analog and a digital part. The mixing of the IF digital data and LO signals is done in the digital part using AND gates and the time division multiplexing of the up-converted signals is done using OR gates. The analog part of the unit cell consists of an LSB size NMOS current source, which is biased by an internal standard beta multiplier bias generator, and a cascode NMOS switch that is controlled by the input

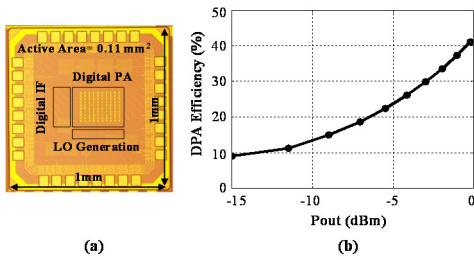


Fig. 5. (a) Die micrograph of the transmitter. (b) DPA efficiency.

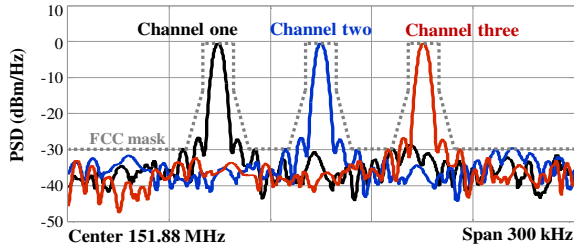


Fig. 6. Measured output spectrum of single-tone BPSK at 5kb/s

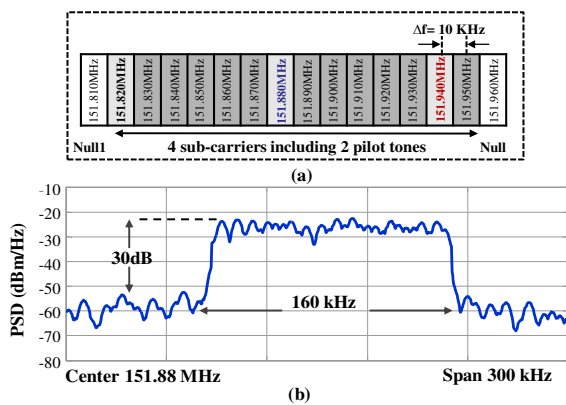


Fig. 7. (a) OFDM modulation frequency planning. (b) Measured close-in PSD of multi-tone MURS transmission at 384kb/s.

digital data. The current source transistors are sized appropriately to maximize the output dynamic range and minimize noise. The 64 unit cells are drain-combined and connected to the output load. Fig. 4(b) shows the floorplan of the segmented DPA and the special switching scheme proposed in this work. The DAC is implemented with a common centroid layout architecture and dummy cells are added to avoid the edge effects. For linearity purposes and in order to mix the input digital signal with the LO signal with the right phase, the digital I/Q mixing and combining, the switches and the current sources are all placed in the same array. Since 64 unit current sources have to be placed in the DAC array and only 32 digital I/Q combining blocks are needed for all the unit cells, two separate types of unit cells are designed. The 32 shaded unit cells include both the analog and digital parts of the DAC, and the other 32 non-shaded unit cells only include the analog part of the DAC together with dummy I/Q combining digital blocks that are

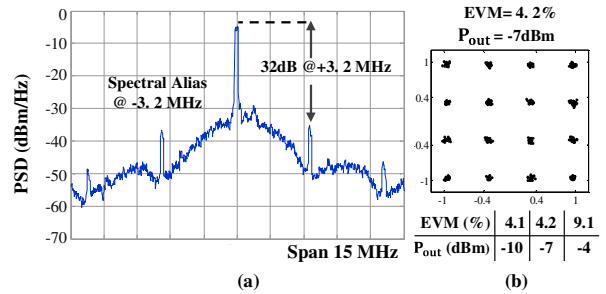


Fig. 8. (a) Far-out PSD of multi-tone transmission (b) EVM and constellation diagram of 160kHz 16QAM symbols.

placed for the symmetry of the layout. The wiring of the 7 bit thermometer and 3 bit binary segments of all four I/Q channels is done accordingly.

The differential  $2 \times$  LO signals at twice the carrier frequency are fed from an external source to an LO generator block shown in Fig. 4(c), which creates the 25% duty cycled LOs using a divide-by-2 circuit and combinational logic. In this design, it is important that the four 25% duty cycled LO signals are synchronized, therefore a careful 32 point custom clock routing implementation is done in the DAC layout using a separate HTree clock distribution for each of the four LO signal phases to ensure a very low skew.

## V. MEASUREMENTS

The transmitter was fabricated in a LP-65nm CMOS process and packaged in a 5x5mm QFN32 package. The transmitter core blocks, not including the I/O pads, occupy an area of  $450 \times 225 \mu\text{m}^2$ . Fig. 5(a) shows the die photo of the transmitter. An off-chip bandpass filter suppresses the harmonics of the up-converted signal and provides the fundamental MURS band signal. The output matching network of the transmitter is designed by a parallel LC tank using a normal size inductor (22nH) which is matched to a high load impedance at the desired MURS frequency band. This, maximizes the peak output power of the DPA, however in order to lower the code dependent compression of the output impedance, a digital pre-distortion technique is required to improve the linearity in this architecture [10]. The standalone measurement results of the DPA efficiency vs. power is shown in Fig. 5(b). The DPA delivers 41% of efficiency at a peak output power of 0dBm after the matching network. The DPA and all the digital blocks in the design are operating from a 1.2V supply voltage. The transmitter is measured with MURS single-tone and multi-tone transmission schemes. The FCC mask together with the power spectral density (PSD) for the BPSK modulated single-tone transmission of the MURS three lower frequencies of 151.820, 151.880 and 151.940MHz with a data-rate of 5kb/s is presented in Fig. 6. It is shown that the signals are below the FCC mask.

TABLE II  
PERFORMANCE SUMMARY AND COMPARISON WITH THE STATE-OF-THE-ART NARROWBAND TRANSMITTERS

Reference	This Work		[6] JSCC16	[11] ISSCC17	[12] JSSC11	[13] RFIC14
Technology	65nm		40nm	65nm	130nm	130nm
Architecture	Digital Class-B I/Q cell sharing		Digital Polar	Digital Polar	Digital Injection-Locked	Analog MUX/ILO
Carrier Freq.	151.82-151.94MHz		750-930MHz	850-920MHz	433MHz	2360-2480MHz
Supply Voltage	1.2V		1V	3.3V	1V	1.5/1V
Modulation	BPSK	16QAM OFDM	64QAM OFDM	UNB DBPSK	BFSK	$\pi/4$ -DQPSK
Data-rate	5kb/s	384kb/s	-	100b/s	200kb/s	971 kb/s
Peak Power	0dBm		8dBm	14.7dBm	-11dBm	-
Peak Efficiency	41%		45%	-	30%	-
Avg. Power	-7dBm		0dBm	10dBm	-17dBm	-10dBm
ACLR	-30dB at 160KHz offset		-	-	-	-33dB
EVM	4.2%		4.4%	<5%	-	3.2%

For the spectrally efficient long range communication mode, the multi-tone transmission in MURS band is measured with a 16QAM OFDM signal discussed in section II. The proposed OFDM frequency planning used for the multi-tone MURS transmission is presented in Fig 7(a). It achieves 384kbps of raw data-rate over 160kHz of bandwidth. The multi-tone transmission is not FCC compliant because it utilizes the white spaces between the MURS band channels for signal, however it is used as a proof of concept for a spectral efficient performance of the DTX over a narrowband OFDM modulation for long-range IoT applications requiring higher data-rates. The measured close-in PSD of the 16QAM, MURS band OFDM modulation with 6.9dB PAPR is shown in Fig. 7(b), which shows an ACLR value of -30dB at 160kHz frequency offset for a transmit power of -7dBm. The average efficiency of the DPA at 7dB back-off power is 19.2%. Based on our link budget analysis for an average transmit power of -7dBm over 160kHz of bandwidth, a line-of-sight coverage range of 4km is achievable assuming a path loss component of 2.

The measured far-out spectrum of 160kHz 16QAM signal is shown in Fig. 8(a) and the spurs are repeated every sampling rate of 3.2MHz. As shown in Fig. 8(b) the RMS EVM at -7dBm output power is 4.2%. At higher output powers the DPA goes to the cut-off region out of the 6.9 dB PAPR range, and the EVM starts to degrade as shown in the table in Fig 8(b). Table II summarizes the measured performance of the transmitter and compares this work to the state-of-the-art narrowband transmitters.

## VI. CONCLUSION

A low power digital quadrature transmitter was presented. By utilizing the MURS frequency planning a low power solution is proposed for wide area coverage for the IoT. The transmitter efficiency is enhanced by employing the digital class-B input codeword profile in combination with the time division multiplexing of the quadrature data. The transmitter delivers a peak efficiency of 41% at a peak output power of 0dBm. This work provides a competitive solution for emerging long range IoT applications.

## ACKNOWLEDGMENT

This work is supported by NSF under award number CNS 1422175.

## REFERENCES

- [1] M. Centenaro *et al.*, "Long-range communications in unlicensed bands: the rising stars in the IoT and smart city scenarios," in *IEEE Wireless Commun.*, vol. 23, no. 5, pp. 60-67, October 2016.
- [2] Semtech Corporation, "LoRa Modulation Basics," tech. rep. AN1200.22, May 2015; <http://www.semtech.com/images/datasheet/an1200.22.pdf>.
- [3] Y. P. E. Wang *et al.*, "A Primer on 3GPP Narrowband Internet of Things," in *IEEE Commun. Mag.*, vol. 55, no. 3, pp. 117-123, March 2017.
- [4] Federal Communications Commission, Electronic Code of Federal Regulations (e-CFR), Title 47, Part 95, Subpart J, Jan. 2017. Available: <https://www.fcc.gov/general/rules-regulations-title-47>.
- [5] D. Kim *et al.*, "Highly efficient and wideband digital quadrature transmitter," *IEEE MTT-S Int. Microwave Symp. Dig.*, Seattle, WA 2013, pp. 1-3.
- [6] A. Ba *et al.*, "A 1.3 nJ/b IEEE 802.11ah Fully-Digital Polar Transmitter for IoT Applications," in *IEEE J. Solid-State Circuits*, vol. 51, no. 12, pp. 3103-3113, Dec. 2016.
- [7] H. Jin *et al.*, "Efficient digital quadrature transmitter based on IQ cell sharing," *IEEE Int. Solid-State Circuits Conf. Dig. of Tech. Papers*, CA, 2015, pp. 1-3.
- [8] M. S. Alavi *et al.*, "A Wideband 2x13-bit All-Digital I/Q RF-DAC," in *Trans. on Microw. Theory Techn.*, vol. 62, no. 4, pp. 732-752, April 2014.
- [9] A. Mirzaei *et al.*, "Analysis and Optimization of Direct-Conversion Receivers With 25% Duty-Cycle Current-Driven Passive Mixers," in *IEEE Trans. on Circuits and Systems I: Regular Papers*, vol. 57, no. 9, pp. 2353-2366, Sept. 2010.
- [10] T. R. Bhat *et al.*, "Design Tradeoffs and Predistortion of Digital Cartesian RF-Power-DAC Transmitters," *IEEE Tran. on Circuits and Systems II: Express Briefs*, vol. 63, no. 11, pp. 1039-1043, Nov. 2016.
- [11] D. Lachartre *et al.*, "A TCXO-less 100Hz-minimum-bandwidth transceiver for ultra-narrow-band sub-GHz IoT cellular networks," *IEEE Int. Solid-State Circuits Conf.*, San Francisco, CA, 2017, pp. 134-135.
- [12] J. Pandey *et al.*, "A Sub-100  $\mu$ W MICS/ISM Band Transmitter Based on Injection-Locking and Frequency Multiplication," *IEEE J. Solid-State Circuits*, vol. 46, no. 5, pp. 1049-1058, May 2011.
- [13] M. Rahman *et al.*, "A 2.5nJ/bit multiband (MBAN & ISM) transmitter for IEEE 802.15.6 based on a hybrid polyphase-MUX/ILO based modulator," *IEEE Radio Frequency Integr. Circuits Symp.*, Tampa, FL, 2014, pp. 17-20.